Ultra Low RCS Measurement Using Doppler Frequency Shift

E. S. Kashani, Y. Norouzi, A. Tavakoli, and P. Dehkhoda

Department of Electrical Engineering, Amirkabir University of Technology, Tehran, Iran
alamkashani@aut.ac.ir, y.norouzi@aut.ac.ir, tavakoli@aut.ac.ir, pdehkhoda@ aut.ac.ir

Abstract **–** A new clutter removal method is proposed for ultra-low RCS measurement in anechoic chamber. In the proposed method, the target is moved along the line of sight of the radar in a sinusoidal manner. This movement generates some Doppler frequency shift. At the receiver, a filter matched to this Doppler shifter signal is implemented digitally. While the matched filter removes clutter signal largely it preserves the echo from the moving target. As it is shown through analytic estimation as well as simulations, the method can attenuate the clutter and noise level far beyond previously suggested methods. It also removes some of the difficulties in higher frequencies that exist in previous methods.

Index Terms **-** Clutter signal, Doppler effect, matched filter, and radar cross section (RCS) measurement.

I. INTRODUCTION

Radar cross section (RCS) is a crucial term in radar equation and the detection range of any radar system changes with the fourth root of the RCS of the target. This fact necessitates the true estimation of the RCS of the target before any radar system design.

While the RCS of simple shapes can be calculated analytically, for most complicated objects the analytical solutions cannot be obtained easily. In such cases, even computer simulation programs are not so helpful since these programs take a lot of time and memory to solve the RCS problem. Therefore, direct RCS measurement methods are the best practical ones to determine the true RCS of these targets. Basically in the methods the target is placed in an anechoic chamber and is illuminated using radar with known parameters (i.e., transmitted power, antenna gain, and system losses). The echo signal is received and processed and the power of this signal is measured. Then the radar equation is used to determine the RCS of the target that is denoted by σ in the following equation [1],

$$\sigma = \frac{P_r}{P_T} \times \frac{(4\pi)^3 R^4 L}{G^2 \lambda^2}. \quad (1)$$

Here P_r and P_T are the received and transmitted powers, respectively. R is the distance from radar phase center to target, L is the radar system loss, G is the radar antenna gain, and λ is the wavelength. While the basic method is capable to estimate the RCS of large objects, one is not sure about its accuracy for small targets. This is because any practical anechoic chamber has some (minor) wave reflection. The reflection is received by radar and is added to that of the object. For small objects, the additional signal may be comparable with target echo and will cause measurement error. Modern design of novel stealth vehicles with reduced radar signatures has made the conventional RCS measurement methods inefficient. Therefore, other methods should be developed to be able to measure much smaller RCS values. Some authors have proposed other methods in order to get better results in estimating the RCS of small objects.

Since the very beginning of radar appearance, estimation of the radar cross section (RCS) of targets has been of great concern to radar designers. Since a 1dB reduction of the RCS of the target yields roughly 6% reduction of radar detection range. While the RCS of simple objects can be calculated using well-defined electromagnetic methods such as method of moments (MOM) [2], or physical optics (PO) [3], it is not easy to find a simple solution for RCS of complex objects. Since then many people have developed different methods for RCS measurement or estimation.

Submitted On: Sept. 29, 2012
Accepted On: Jan. 27, 2014

One of the primary and basic methods of RCS measurements is to illuminate the target with nano-second pulses and measure the power of the reflected echo [4], this measurement should be done in an anechoic chamber. The necessary conditions for such an anechoic chamber have been presented in [5]. Although the nano-second pulse method is simple in theory, it needs a high power transmitter as well as a large anechoic chamber. The above deficiencies have led to find some simpler measurement methods such as linear FM (LFM) [6] or stepped frequency methods [7]. Also in [8], Polcrass has described the implementation of stepped frequency method with low PRF pulses to achieve the RCS estimation for big objects. Schöne and Riegger have described in [9] how a vector network analyzer can be used to measure the RCS of targets by using FMCW or stepped frequency stimulation. Kent in [10] has described some calibration targets to be used for RCS measurement device calibration. The accuracy of the RCS measurement methods is evaluated in [11]. A review of all basic RCS measurement methods can be found in [12].

Many RCS measurement researches concentrate on polarimetric RCS estimation [13]. In [14], Sarabandi and his team have developed a polarimetric RCS measurement by using single antenna. Muth in [15] and Welsh, Kent and Buterbugh in [16], have described a calibration method for such a task.

Large chambers are required for many ordinary RCS measurements but they are not accessible in many cases. To overcome this difficulty some authors have concentrated on RCS measurement techniques for small chambers [17, 18], and on near field to far field transformation [19]. In [20] Broquetas and Palau have produced a planar wave in a small chamber by using an offset parabolic reflector. Much of the recent research about RCS measurement has been concentrated on clutter and noise removal in order to achieve result that is more accurate. In [21] Hantscher and Diskus have developed a wide band noise reduction method for accurate RCS measurement. In [22] target moved along the line of sight and the change in the phase of reflected echo is used in an LMS estimation returned process to remove clutter contaminations from signal. In [23] Broquetas and Palau have suggested inverse synthetic aperture radar (ISAR) processing methods to remove the clutter signal during target RCS measurement. Finally, Burns and Subotic in [24] have proposed independent component analysis (ICA) for clutter removal from target echo signal.

In this paper, we propose a clutter reduction method based on Doppler frequency shift and matched filter concept. The combination of our method with previous ones can reduce the noise and clutter signal drastically, so enables the system to estimate the RCS of ultra-small objects.

The paper is organized as follows: In section II, basic low RCS measurement methods are presented and their difficulties are expressed from [7, 25, 26]. In section III, we present our new method and apply it to a concrete case. In section IV, the method is simulated in order to evaluate its performance under more realistic conditions. The final section gives the conclusion and some suggestions for more research.

II. BASIC CLUTTER REMOVAL METHODS

While different authors have presented different RCS measurement methods, not all methods are capable to measure the RCS of ultra- small object. In this section, we will study the methods applicable for ultra-small object. The most well-known low radar cross section measurements are as follows.

A. Time gating in step frequency method

In step frequency continuous wave measurement, RCS is measured at many different frequencies, and inverse Fourier transform (IFFT) is used to convert frequency samples to time (range). The time (range) profile helps us to eliminate signals not equidistance to the antenna as the target. This elimination is called time gating. As it is shown in [7], by using the time gating, all clutters that are not equidistant with target to the radar would be removed. But equidistant clutters cannot be removed.

B. Coherent background subtraction method

In CBS method, a background RCS measurement is made over the desired frequency band in the empty chamber, then the target is placed in the chamber and the measurement is repeated. If the scattering vector (phase and amplitude) of the first stage is subtracted from the scattering vector of the second one at each

measured frequency and aspect angle, the result is the right target's signal. As it is shown in [25] this method have several difficulties especially at higher microwave frequencies.

C. Direct path signal removal method

The principle of the method as it is shown in [26] is the same as the background subtraction method. One can see the structure of the method in Fig. 1.

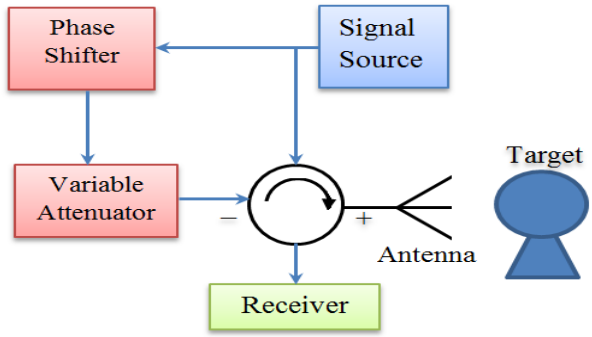

Fig. 1. System block diagram for direct path signal removal method.

In the method with no target in anechoic chamber, the attenuator and the phase shifter is adjusted so that at the output of the power combiner just noise can be detected. In the next step, target is placed in chamber and in this case, the signal received from the collector is the target's RCS. In this method, the same difficulty appears as in the background subtraction method. Therefore, in high frequencies, it cannot be applied. Also because of the restricted dynamic range of the phase shifter and attenuator, clutter cancellation cannot be done properly. Therefore, the method cannot achieve high dynamic ranges.

III. THE METHOD BASED ON DOPPLER FREQUENCY SHIFT

Figure 2 shows the structure of the proposed method. In the below design, the following methods are used simultaneously to reduce the existing clutter: direct path signal removal, time gating clutter removal, and Doppler frequency shift effect.

In the following, all previous methods are formulated and the level of clutter removal is determined.

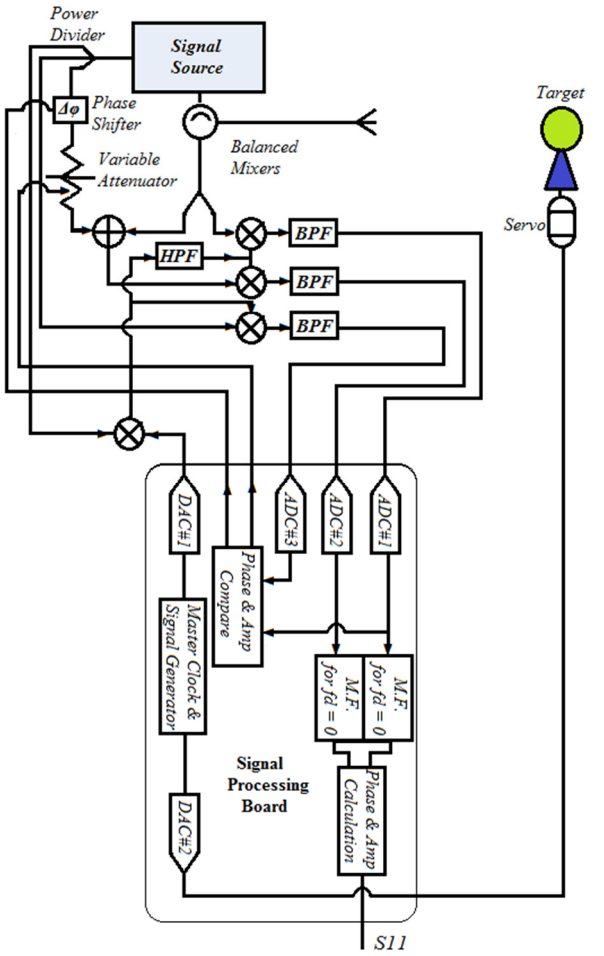

Fig. 2. System block diagram of Doppler frequency shift method.

A. Direct Path signal removal

As it can be seen in Fig. 2 signals of ADC #2 and ADC #3, are compared, and the subtraction of phases and amplitudes calculated, while target is placed at a fixed position. In this case, depending on gotten vector, direct path signal is attenuated and phase shifted and added to the signal received from the antenna. Ideally, one should get zero amplitude from the sum. However, in practice, because of some errors in the phase and amplitude estimation and also phase shifter and attenuator adjustment, the result is not zero. The errors in phase and amplitude estimation can be reduced by lengthening the observing interval and calculating long-term FFT. However, the errors in the phase shifter, attenuator adjustment, and time averaging still remain. If the first step of attenuator and phase shifter (which have least amount) are equal to Δa and $\Delta \varphi$,

respectively, then the output of collector is equal to,

$$x = \cos wt - \Delta a \cos(wt + \Delta\varphi)$$
$$x = (1 - \Delta a \cos \Delta\varphi) \cos wt + \Delta a \sin \Delta\varphi \sin wt = A \cos(wt + \psi) \quad . \tag{2}$$

Here A and ψ are equal to,

$$A = \sqrt{(1 - \Delta a \cos \Delta\varphi)^2 + \Delta a^2 (\sin \Delta\varphi)^2} = \sqrt{1 + \Delta a^2 - 2\Delta a \cos \Delta\varphi} \tag{3}$$

$$\psi = \tan^{-1}\left(\frac{\Delta a \sin \Delta\varphi}{1 - \Delta a \cos \Delta\varphi}\right). \tag{4}$$

The amplitude of the remained signal (i.e., A) related to the original signal is presented in Fig. 3. Figure 3 shows that for any value of Δa and small values of $\Delta\varphi$, the attenuation level tends to,

$$A = 1 - \Delta a. \tag{5}$$

Usually in practical systems, one cannot get Δa, to be less than 0.25 dB. Therefore referring to Fig. 3, direct path signal removal method attenuates clutter at most 30dB.

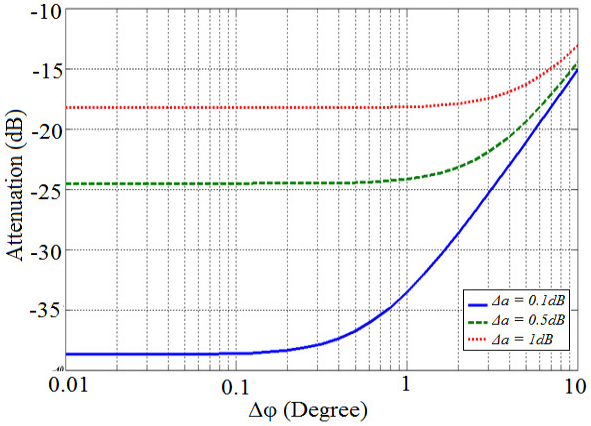

Fig. 3. Clutter removal level as a function of attenuation and phase shift steps.

B. Time gating clutter removal

In time gating method RCS measurement is done with different frequencies and at each frequency, phasor of scattered signal is obtained. However, it is shown in [27], with the use of inverse Fourier transform of these phasors, time domain profile is extracted and scattering from different points is decomposed. Actually if the number of frequencies equal to N and separation frequency equals ΔF, signals are mapped with resolution of $\frac{c}{2N\Delta F}$ meter between 0 to $\frac{c}{2\Delta F}$ meter. It means that clutter is divided into N parts and just one of them is equidistant to the target and that one will remain. Therefore, if we imagine that the clutter signal is homogenous then the method attenuates the clutter N times. However, if the clutter signal is not homogenous and no part of the signal is equidistant with the target to the radar, then the attenuation rate is more than that.

C. Doppler frequency shift effect

In Doppler frequency shift method, the target that is mounted on special pylons starts to move back and forth along the radar line-of-sight. The movement has a sinusoidal pattern with total displacement equals to 2Δx and angular frequency equals to ω_m. Then with $\Delta x \ll R$ (R is the mean distance of the target to antenna) the received signal is as follows,

$$S(t) = A_T \cos(w_c(t - \frac{\Delta x}{c} \cos \omega_m t)). \tag{6}$$

The signal is brought to the IF band, which is equal to,

$$S_{IF}(t) = A_T \cos\left(w_{IF} t - \frac{\Delta x . w_c}{c} \cos(\omega_m t)\right). \tag{7}$$

Scattered echo of stationary targets (i.e., clutter) in IF band is equal to,

$$S_c(t) = A_c \cos(w_{IF} t). \tag{8}$$

Now both target and clutter signals are passed through the filter that is matched to the echo of the moving target. The Impulse response of the matched filter equals,

$$h(t) = S_{IF}(T_s - t). \tag{9}$$

Here T_s is the total observation (sampling time). While passing through the matched filter, target echo will increase and the clutter signal is attenuated considerably. Figure 4 shows amplitude of the matched filter output for a target and a clutter with the same RCS. Here Δx equals 10 cm, f_m=10 Hz, and f_c=10 GHz.

It is easy to show that the clutter removal depends on $\Delta x/\lambda$, ω_m, T_s and maximum distance of the targets (maximum delay). However, it is not easy to extract a simple (closed form) equation for attenuation level, in Fig. 5, Monte-Carlo simulation method is used to find this attenuation level. In the simulations the chosen T_s equals to 10 second, τ_d=10 microsecond, $0.1 < \frac{\Delta x}{\lambda} < 10$ and ω_m =0.1 or 1 or 10.

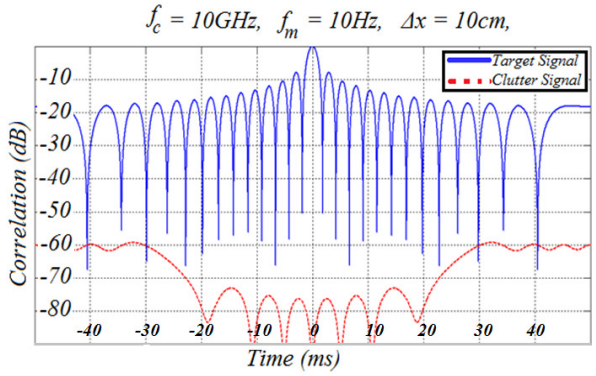

Fig. 4. The target and clutter signals at the output of matched filter (the target and the clutter have the same RCS).

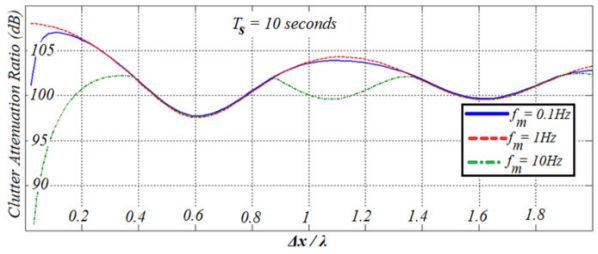

Fig. 5. Clutter removal level as a function of the frequency and the range of target movements (10 seconds signal integrations).

As it is seen in Fig. 5, the maximum target displacement should be at least one tenth of the wavelength. But the bigger Δx will not improve the attenuation level substantially, and the oscillation frequency does not have a great impact on the clutter removal performance of the system. The figure just shows that for Δx larger than one tenth of a wavelength, the clutter removal is about 100 dB.

In Fig. 6 the scenario is repeated with T_s = 1sec. It can be seen that 0.1 Hz oscillation frequency is not desirable anymore. Referring to this case if Δx almost equals two tenth of the wavelength, then the clutter removal level would be about 80 dB.

IV. SIMULATION RESULTS

In this section, the proposed Doppler processing method is simulated in some ideal and also practical cases. The results are compared against the theoretical values obtained in section III. In these simulations, 21 point-scatterers are assumed to be placed from 3 meters to 5 meters from the transmitting antenna. The RCS of these scatterers are assumed to be random valued with an exponential distribution. The mean RCS of each point scatterer equals 10^{-2} m^2. The target is also assumed to be a point scatterer with an RCS equals to 10^{-7} m^2. The distance between the target and the transmitting antenna is four meters, and the target vibrates about ±5 cm around this point in each 100 milliseconds.

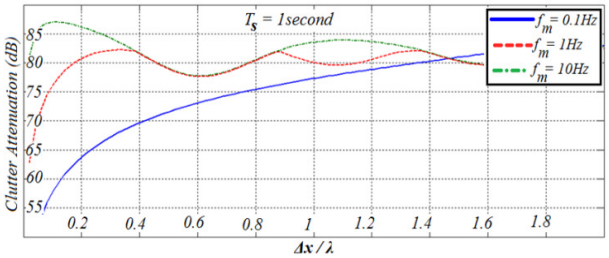

Fig. 6. Clutter removal level as a function of the frequency and the range of target movements (one second signal integrations).

The measurement system includes a frequency synthesizer operating from 8 GHz to 12 GHz (X-band), an antenna with 15 dBi gain, and a power amplifier that produces 1 milliwatt (0 dBm) at its output. The received signal is down converted to 1 kHz and is filtered with a narrow 100Hz band pass filter. The signal is sampled at 10 kilo-sample-per-second (ksps). The samples are collected for the duration of 10 seconds, then the proposed Doppler process in the previous section is carried out to extract target signal from that of the clutter.

In Fig. **7**, the power of the received signal at different frequencies is sketched before and after Doppler process. These two graphs are compared to the one that is obtained if just the target is under system illumination. As it is seen, before the process, the graph mainly represents the clutter's echo and there is no similarity between the power of the received signal and that of the right target. However, after Doppler processing there is a great coincidence between the processed signal and the true signal values. Based on Fig. 7, the clutter to signal power ratio (CSR) before and after Doppler processing is shown in Fig. 8. As it is observed, while in the raw signal the clutter is 50 dB more powerful than the target signal on average, after the process this ratio decreases roughly to -70 dB. This fact shows that the Doppler processing

method reduces the clutter signal at about 120 dB. The attenuation value is more than the one estimated in the previous section. This is because the clutter is just one point scatterer while in the simulations the clutter consists of 21 point scatterers.

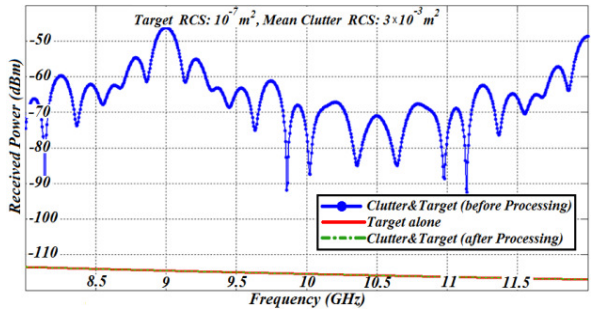

Fig. 7. Amplitude of received signal at different frequencies, before and after Doppler process (the Target alone (red) and the Clutter &Target after processing (green) curves have negligible differences and these curves are almost jugate).

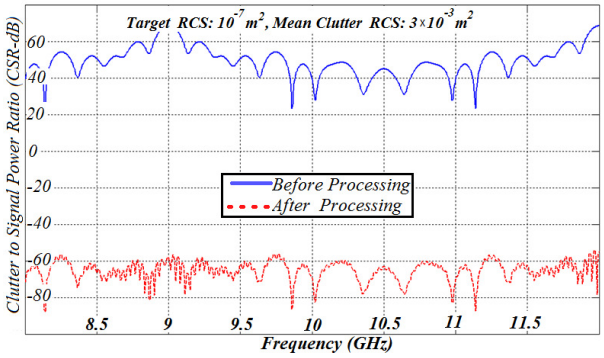

Fig. 8. Clutter to signal power ratio (CSR) before and after Doppler processing.

In the previous simulation an ideal receiver was assumed. However, in practical cases the system suffers from noise and impurities. In what follows the noise and impurity effects have been considered in order to evaluate the performance of the method under some more realistic conditions.

In Fig. 9 simulated model includes thermal noise effect. As it is observed, while at 20dB SNR value an error about 15dB may exist in the predicted received signal, for 30dB SNR, this error will be reduced to less than 5 dB. At 40dB SNR value, on average less than 1dB error will be observed.

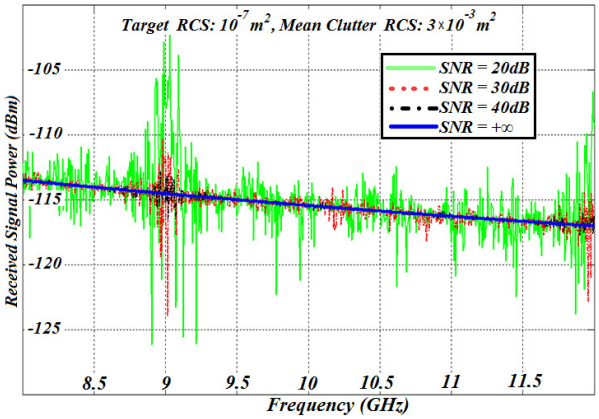

Fig. 9. Effect of input signal to noise ratio on the estimated target's received power.

In Fig. 10 the effect of quantization noise is simulated. Referring to this figure, the noise generated about 1dB error in the estimated signal's received power. It is amazing to observe that the average error is not strongly related to the total number of quantization bits.

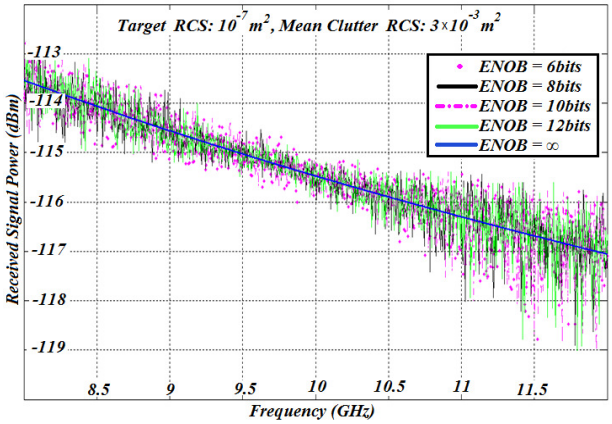

Fig. 10. Effect of quantization noise on the estimated target's received power.

Finally in Fig. 11, the effect of local oscillator impurity is simulated. As it is observed, while 10 degrees phase jitter produce a considerable error on the estimated targets received signal, the effect of impurity will become almost ignorable if the rms phase jitter is reduced to 1degree.

V. CONCOLUSION

In the paper, a new combined method for ultra-low RCS targets has been proposed. We see that with the help of direct path signal removal method, the clutter elimination is between 35 to 45 dB. In

addition, we see that Doppler frequency shift removed clutter between 80 dB to 100 dB. Clutter removal using time gating equals the number of the frequencies. If we have 100 to 1000 frequencies, then clutter attenuation is between 20 to 30 dB. Finally, by the use of the three methods together one can remove clutter 135 dB to 175 dB. This is much better than the previous methods. Of course, we should be aware that when this rate of clutter removal is used, problems like phase noise of oscillators and number of ADC bits will appear. By using simulations, it is shown that the effect of the thermal noise, quantization noise, etc., is so small that can be ignored.

It should be remembered that in our method the signal reflected from the moving part of the mount has the same Doppler nature as the target. So the new method cannot remove this part of the clutter. Regarding this fact, the moving part of the mount should be made of low RCS materials. Also direct signal removal can be used to omit this part of the clutter. However, for very low RCS measurement, more elaborated methods should be found to eliminate the deficiency of the method.

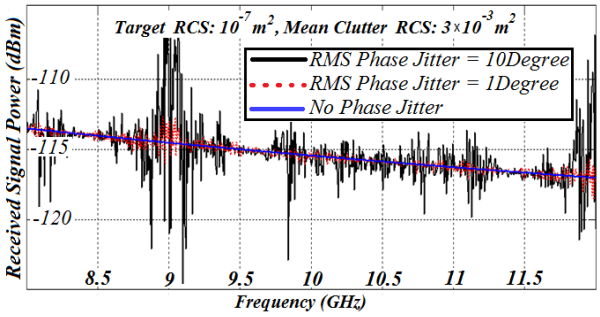

Fig. 11. Effect of local oscillator impurity on the estimated target's received power.

REFERENCES

[1] M. Skolnik, *Radar Handbook*, Third Edition, McGraw-Hill Professional, January 2008.

[2] M. O. Sadiku, *Numerical Techniques in Electromagnetics*, 2nd edition, CRC Press, 2000.

[3] C. A. Bennett, *Principles of Physical Optics*, first edition, Wiley, January 2008.

[4] C. G. Bachman, "Some recent developments in RCS measurement techniques," *Proceedings of The IEEE*, vol. 53, no. 8, pp. 962-974, August 1965.

[5] B. K. Chung, H. T. Chuah, and J. W. Bredod, "A microwave anechoic chamber for radar- cross section measurement," *IEEE Antennas and Propagation Magazine,* vol. 39, no. 3, pp. 21-26, June 1997.

[6] R. T. Lawner, P. F. Blanchard, and S. Gogineni, "Coherent FM-CW millimeter-wave radar systems for radar cross section measurements," *IEEE Transactions on Instrumentation and Measurement*, vol. 39, no. 1, pp. 208-211, February 1990.

[7] P. S. Kao, "Automated step frequency radar cross section measurements," *Antennas and Propagation Society International Symposium*, vol. 20, pp. 237-240, 1982.

[8] R. M. Polcrass, "Radar cross section measurements using target striping," *Telesystems Conference*, vol. 1, pp. 183-186, 1991.

[9] G. Schöne, S. Riegger, and E. Heidrich, "Wideband polarimetric radar cross section measurement," *Antennas and Propagation Society International Symposium*, vol. 2, pp. 537-540, 1988.

[10] B. M. Kent, "Comparative measurements of precision radar cross section (RCS) calibration targets," *IEEE Antennas and Propagation Society International Symposium*, vol. 4, pp. 412-415, 2001.

[11] B. M. Welsh and J. N. Link, "Accuracy criteria for radar cross section measurements of targets consisting of multiple independent scatterers," *IEEE Transactions on Antennas and Propagation*, vol. 36, no. 11, pp. 1587-1593, November 1988.

[12] T. E. Tice, "An overview of radar cross section measurement techniques," *IEEE Transactions on Instrumentation and Measurement*, vol. 39, no. 1, pp. 205-207, February 1990.

[13] K. Sarabandi and F. T. Ulaby, "A convenient technique for polarimetric calibration of single antenna radar system," *IEEE Transactions on Geoscience and Remote Sensing*, vol. 28, no. 6, pp. 1022-1033, November 1990.

[14] J. J. Ahne, K. Sarabandi,, and F. T. Ulaby, "Design and implementation of single antenna polarimetric active radar system," *Antennas And Propagation Society International Symposium*, vol. 3, pp. 1280-1283, 1993.

[15] L. A. Muth, "Nonlinear calibration of polarimetric radar cross section measurement systems," *IEEE Antennas and Propagation Magazine*, vol. 52, no. 3, pp. 187-192, June 2010.

[16] B. M. Welsh, B. M. Kent, and A. L. Buterbaugh, "Full polarimetric calibration for radar cross-section measurements performance analysis," *IEEE Transactions on Antennas and Propagation*, vol. 52, no. 9, pp. 2357-2365, September 2004.

[17] O. M. Bucci and M. D. Migliore, "Effective estimation of 2-D monostatic radar cross sections

from Near-Field measurements," *IEEE Transactions on Antennas and Propagation*, vol. 54, no. 2, pp. 750-752, February 2006.

[18] J. W. Odendaal and J. Joubert, "Radar cross section measurements using near-field radar imaging," *IEEE Transactions on Instrumentation and Measurement*, vol. 45, no. 6, pp. 948-954, December 1996.

[19] C. R. Birtcher, C. A. Balanis, and V. J. Vokurka, "RCS measurements, transformations, and comparisons under cylindrical and plane wave illumination," *IEEE Transactions on Antennas and Propagation*, vol. 42, no. 3, pp. 329-334, March 1994.

[20] A. Broquetas, J. Palau, L. Jofre, and A. Cardama, "Spherical wave near-field imaging and radar cross section measurement," *IEEE Transactions on Antennas and Propagation*, vol. 46, no. 5, pp. 730-735, May 1998.

[21] S. Hantscher, A. Reisenzahn, and C.G. Diskus, "Ultra-wide band radar noise reduction for target classification," *IET Radar Sonar and Navigation*, vol. 2, no. 4, pp. 315-322, 2008.

[22] L. A. Muth, C. M. Wang, and T. Conn, "Robust separation of background and target signals in radar cross-section measurements," *IEEE Transactions on Instrumentation and Measurement*, vol. 54, no. 6, pp. 2462-2468, December 2005.

[23] A. Broquetas, J. Palau, L. Jofre, and A. Cardama, "Spherical wave near-field imaging and radar cross-section measurement," *IEEE Transactions on Antennas and Propagation*, vol. 46, no. 5, pp. 730-735, May 1998.

[24] J. W. Burns and N. S. Subotic, "Reduction of clutter contamination in radar cross section measurements using independent components analysis," *IEEE Antennas and Propagation Society International Symposium*, vol. 1, pp. 731-734, 2004.

[25] A. Bati, T. Long, and H. Don, "Advanced radar cross section clutter removal algorithms", *Antennas and Propagation (EuCAP), 2010 Proceedings of the Fourth European Conference*, pp. 1-5, 2010.

[26] M. Miacci, I. Martin, and M. Rezende, "Radar cross section measurements of complex targets (missile parts) in C-band in anechoic chamber," *Microwave and Optoelectronics Conference, IMOC 2007. SBMO/IEEE MTT-S International*, pp. 401-405, 2007.

[27] N. Levanon and E. Mozeson, *Radar Signals*, first edition, Wiley-IEEEPress, July 2004.

Elham Sadat Kashani received the B.Sc. degree from Sharif University of Technology, Tehran, Iran, and the M.S. degree from the Amirkabir University of Technology, Tehran, Iran, both in electrical engineering. Her research interests include radar signal processing and modeling.

Yaser Norouzi (born in 1981) achieved his B.Sc, M.Sc, and PhD in Communication systems in 2001, 2003, and 2007, respectively all from Sharif University of Technology, Tehran, Iran. Currently he is with Department of electrical engineering at AmirKabir University of technology, Tehran, Iran. His fields of interest include analyzing of dynamic systems, Game Theory and Stochastic Processes.

Ahad Tavakoli was born in Tehran, Iran, on March 8, 1959. He received the B.S. and M.S. degrees from the University of Kansas, Lawrence, and the Ph.D. degree from the University of Michigan, Ann Arbor, all in electrical engineering, in 1982, 1984, and 1991, respectively. In 1991, he joined the Amirkabir University of Technology, Tehran, Iran, where he is currently a Professor in the Department of Electrical Engineering. His research interests include scattering of electromagnetic waves, electromagnetic compatibility, and microstrip antennas.

Parisa Dehkhoda received the B.S. degree from Tehran University, Tehran, Iran, and the M.S. and Ph.D. degrees from the Amirkabir University of Technology, Tehran, Iran, all in electrical engineering. She is currently an Assistant Professor in the Institute of Communications Technology and Applied Electromagnetics, Amirkabir University of Technology, Tehran, Iran. Her research interests include electromagnetic compatibility, specially shielding enclosures, scattering of electromagnetic waves and microstrip antennas.